Laser Spectroscopy

International Edition: DOI: 10.1002/anie.201502591
German Edition: DOI: 10.1002/ange.201502591

Optical Absorption and Magnetic Field Effect Based Imaging of Transient Radicals**

*Joshua P. Beardmore, Lewis M. Antill, and Jonathan R. Woodward**

Abstract: *Short-lived radicals generated in the photoexcitation of flavin adenine dinucleotide (FAD) in aqueous solution at low pH are detected with high sensitivity and spatial resolution using a newly developed transient optical absorption detection (TOAD) imaging microscope. Radicals can be studied under both flash photolysis and continuous irradiation conditions, providing a means of directly probing potential biological magnetoreception within sub-cellular structures. Direct spatial imaging of magnetic field effects (MFEs) by magnetic intensity modulation (MIM) imaging is demonstrated along with transfer and inversion of the magnetic field sensitivity of the flavin semiquinone radical concentration to that of the ground state of the flavin under strongly pumped reaction cycling conditions. A low field effect (LFE) on the flavin semiquinone–adenine radical pair is resolved for the first time, with important implications for biological magnetoreception through the radical pair mechanism.*

Short-lived radical intermediates are common in a wide range of thermal and photochemical enzyme catalyzed chemical reactions. To date, however, there do not exist microscopic methods for their direct observation. Furthermore spin-correlated radical pairs (RPs) have been extensively studied for the last four decades.[1–3] In recent years they have returned to the spotlight, primarily due to their proposed role in animal magnetoreception,[4] their importance in solid-state devices involving electron–hole recombination[5] and renewed interest in quantum information related phenomena in the physics community. Surprisingly, with few exceptions,[6] the study of RPs in a spatially resolved manner has been largely ignored. In recent years, a range of sophisticated fluorescence-based microscopy methods have been developed and have received much attention.[7] However, fluorescence is not an ideal method for the study of photochemically generated radicals or RPs. Photochemically generated free radicals in general do not fluoresce. Furthermore, although there are many examples of the use of fluorescence detection to study RP dynamics,[1–3] such measurements are typically only possible in spin-selective reactions from singlet RPs to fluorescing exciplexes. In particular, to study RPs proposed in biological magnetoreception, an alternative approach is desirable. In functioning cryptochrome photochemistry, electron transfer to the photoexcited singlet state of FAD (from a neighboring tryptophan residue) is sufficiently rapid to make fluorescence signals extremely weak. In addition, fluorescence only tracks ground state FAD molecules, whose concentration is not magnetic field-sensitive in flash photolysis experiments. In general, transient absorption spectroscopy is the best optical spectroscopic method for studying transient radicals and RPs.

Here, we demonstrate for the first time a new imaging microscope (TOAD) that can observe photochemically generated radicals and RPs with high sensitivity and sub-micrometer spatial resolution, paving the way for the direct measurement of, for example, flavin photochemistry in cells and tissues, and localized polaron pairs in solid-state devices.

The TOAD/MIM microscope is described only briefly here. Full technical details will be published elsewhere. The optical arrangement is based on an instrument for detecting single molecules,[8,9] and employs a transmission confocal arrangement. Two solid-state lasers act as pump and probe. The output of the 532 nm (probe) laser, used for imaging detection, is beam-split before being combined with the output of the 450 nm (pump) laser. The combined beams enter the microscope objective through a single mode optical fiber. The major microscope components comprise a piezoelectric sample translation stage, two apochromatic objective lenses, optical filters/dichroic mirrors and micrometer adjusted translation stages. The microscope is assembled on a vibrationally isolated optical bench to eliminate spurious signals from vibrations, particularly at the audio frequencies used for signal modulation. The output of the upper objective can be directed onto an imaging camera for alignment purposes, or onto the input of an auto-balanced photodetector. The reference for the balanced detection is provided by the split output of the probe laser. Using this method it is possible to reduce fluctuations in laser intensity by >50 dB and the signal becomes shot noise limited. The output of the photodetector is applied to the input of a lock-in amplifier, allowing the sensitive detection of very small changes to the probe beam intensity.

Pump light modulation imaging: The basic imaging technique (TOAD) employs pump laser modulation and monitoring of the induced modulation in the probe beam whilst the lasers are scanned in up to three dimensions over the sample. In the simplest arrangement, square wave modulation is applied to the 450 nm pump laser at an audio frequency. This allows long timescale reaction cycling in flavin photoreactions to be probed directly when the light-on cycle is long enough to allow ground state FAD and RP concentrations to reach equilibrium. The equilibrium position can then be controlled with the pump laser power.

[*] Dr. J. P. Beardmore, L. M. Antill, Prof. J. R. Woodward
Graduate School of Arts and Sciences, The University of Tokyo
3-8-1 Komaba, Meguro-ku (Japan)
E-mail: woodward@global.c.u-tokyo.ac.jp

[**] The authors are grateful for a MEXT scholarship for L.M.A. This work was supported by JSPS KAKENHI Grant Number 24350002.

The microscope objectives employed allow high laser intensities to be produced at the focal point of the microscope, corresponding to FAD photoexcitation rate constants of up to ca. $10^8\ s^{-1}$. Under these conditions, continuous pumping of the sample is capable of significant FAD ground state (GS) photobleaching. By applying short (ca. 300 ns) TTL pulses to the modulation input of the pump laser, the experiment can be operated in flash photolysis mode, and high modulation frequencies (1–100 kHz) can be employed when reaction kinetics are sufficiently fast. Under such conditions, time-resolved optical absorption kinetic curves can be digitized from the photodetector or the signal from the lock-in can be used for imaging or MARY (magnetically affected reaction yield) curve acquisition.

A custom-built Helmholtz coil pair aligned to apply a DC + AC magnetic field co-axial to the optical axis is driven by a 4-pole power supply. The direct effect of the magnetic field on the decay kinetics or modulated signal can be recorded or alternatively, a double modulation scheme can be employed.

Pump light, magnetic field double modulation measurements: For flash photolysis type irradiation, the output of the lock-in can be applied to a second lock-in amplifier, referenced to a sine wave modulation signal (frequency to ca. 1 kHz), used to drive an AC magnetic field at the sample. Monitoring the output of this second lock-in as the laser beams are scanned over the sample, allows the direct recording of a magnetic intensity modulation (MIM) image when the AC magnetic field is combined with a static DC field (tuned to observe the maximum signal). A simple demonstration of this technique is provided here, but its true potential will be fully unlocked in future studies.

MFEs on the RP generated by the photoexcitation of FAD at low pH have previously been reported.[10,11] Electron transfer takes place from the adenine to the flavin moiety generating a separated biradical. Low pH is necessary to stop the two moieties stacking, which facilitates rapid forward and backward electron transfer.[11] Unusually this system appears to involve an equilibrium between RP and protonated FAD triplet state (PTS). Both transient species absorb light at 532 nm with almost equal extinction coefficients. Typical RP/PTS lifetimes under these conditions are a few microseconds.

Figure 1 a shows an image of a ca. 2.5 μm microbead surrounded by 200 μM FAD in pH 2.3 buffer in flash photolysis mode. The sample thickness is bead limited (i.e. < 3 μm) and the lasers irradiate a sample volume of < 4 femtoliters (fL) with a beam waist of ca. 240 nm. The signal used for imaging is a direct measure of RP concentration and is reduced to near zero in the region of the bead as no photochemistry can occur in this region. Figure 1 b shows the time decay following photoexcitation and the subtracted curves recorded in the presence and absence of a 20 mT magnetic field (inset), at a single pixel position away from the microbead. The black line is a numerical simulation employing the kinetic model and parameters described in reference [11]. Such kinetic curves can be obtained at any sample location (the sample stage can access submicrometer horizontal spatial regions) and so could be used to target particular sub-cellular structures to observe flavin photochemistry therein. Figure 1 c shows a MARY curve recorded again at a single point within the sample. Only 8 min was required to record a MARY spectrum at this signal-to-noise level. The vertical scale of the MARY curve is the percentage change in the output of the lock-in signal as the field is scanned.

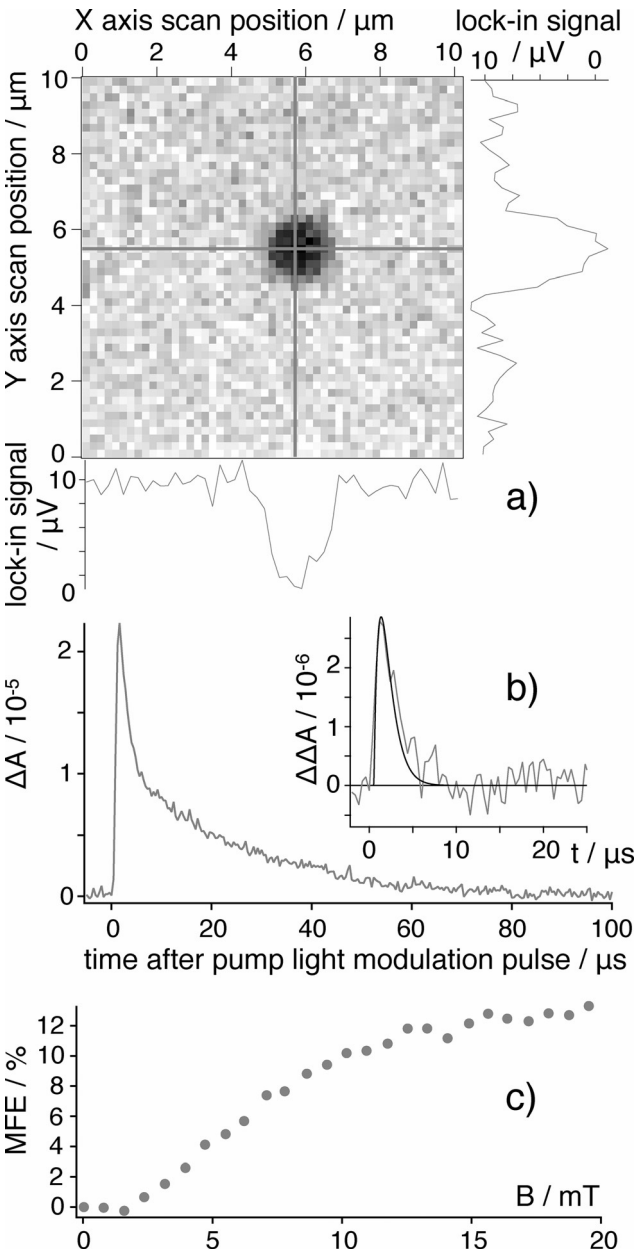

Figure 1. a) Pump light modulation image of FAD semiquinone radicals in the presence of a 2.5 μm microbead generated from 200 μM FAD. Horizontal and vertical slices are shown. b) 532 nm absorption kinetics recorded at a single location. The inset shows subtracted field on/off curves with a simulation based on Ref. [11]. c) Pump light modulation MARY curve recorded at the same location. The sample (1 μL) was < 3 μm thick.

Figure 2 a shows a double modulation image for a slightly larger microbead, this time in 1 mM FAD in pH 2.3 buffer. This is an example of the MIM technique—a non-zero signal is only observed if the probe beam light is absorbed by

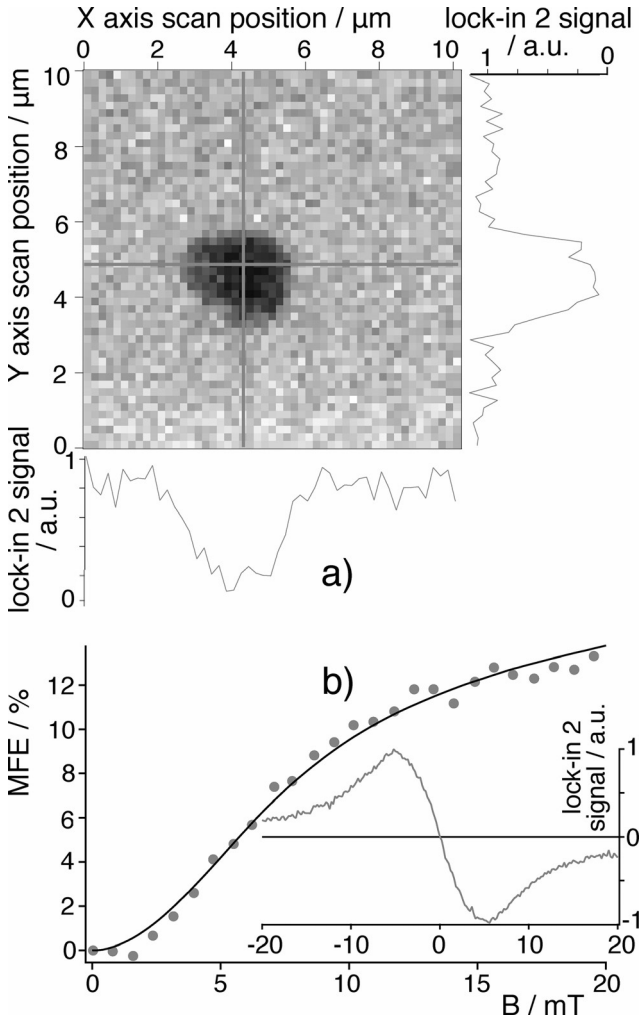

Figure 2. a) Double modulation image of 2.9 µm microbead. b) Inset shows the double modulation MARY curve at a single pixel position. The main curve shows the inset signal integrated and overlaid on the MARY curve from Figure 1 c (dots).

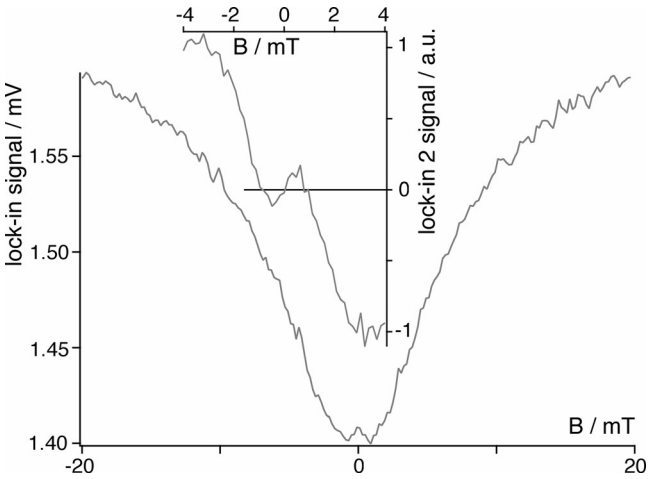

Figure 3. Single (main) and double modulation (inset) MARY curves revealing and confirming the presence of a LFE (5 µL sample with 100 µm glass beads).

a magnetically sensitive species. The inset of Figure 2 b shows a typical double modulation-MARY signal obtained at any point in the image. The characteristic first derivative MFE signal is observed. For the image, the DC component of the applied field was matched to the peak of this MARY signal. Figure 2 b shows the compatibility between the single and double modulation techniques. The integrated double modulation MARY signal (line) overlaps perfectly the MARY curve from Figure 1 c (dots).

By acquiring single (Figure 3, main) and double (Figure 3, inset) modulation MARY curves at a greater magnetic field resolution (and a suitably small MF modulation depth of 0.35 mT peak-to-peak in the double modulation case) it was possible to successfully resolve and confirm a LFE. Although this reaction has been carefully studied by conventional[10,11] and high-sensitivity cavity enhanced techniques,[12] this LFE has not previously been resolved. This reveals the high sensitivity of this approach, which detected the feature using a sample volume of only 5 µL and a second lock-in time constant of only 300 ms. If flavin-based RPs are responsible for biological magnetoreception, then the LFE represents the most likely mechanism by which fields as small as the geomagnetic field (30–50 µT) might deliver a chemical response.

For animals navigating in the geomagnetic field, exposure to light is continuous rather than the series of short nanosecond pulses typical in photochemical kinetic measurements. Our approach allows the observation of MFEs on the equilibrium established between RPs and FAD GS molecules by the use of square wave pump light modulation at variable modulation frequencies and laser powers. For CW irradiation at low pump powers, MFEs are observed in agreement with the effects seen in flash photolysis measurements. As the pump light power is raised the equilibrium shifts towards the RP/PTS state (Figure 4 a and the equation in Figure 4 c) and the size of the MFE gradually diminishes. Figure 4 b demonstrates the effect of increasing the length of the pump laser pulse width from 300 ns to 2000 ns. As the pulse length increases, the complete reaction cycle can occur during the irradiation period, establishing the GS–RP/PTS equilibrium and pushing it in the direction of the RP/PTS due to the intensity of the laser beam. Thus the MARY curves saturate at increasingly low MFE values.

Concomitant with the reduction of the MFE in the RP, the concentration of FAD GS becomes limited by spin-selective back electron transfer from the singlet RP and should thus exhibit an MFE in the opposite sense to that observed in the RP (i.e. a magnetic field should reduce the fluorescence intensity). In order to monitor the concentration of FAD GS, the probe light was removed and the microscope configured to detect the fluorescence signal from excited singlet state FAD. Figure 4 c shows the MARY curve obtained for a square wave pump light modulation measurement with the pump intensity tuned such that the FAD fluorescence is weak enough to reveal the MFE on the FAD GS/excited singlet state, but still sufficiently large to be measureable. The inverted MFE on fluorescence is clearly observed. Thus the field sensitivity of FAD derived triplet borne RPs can exhibit

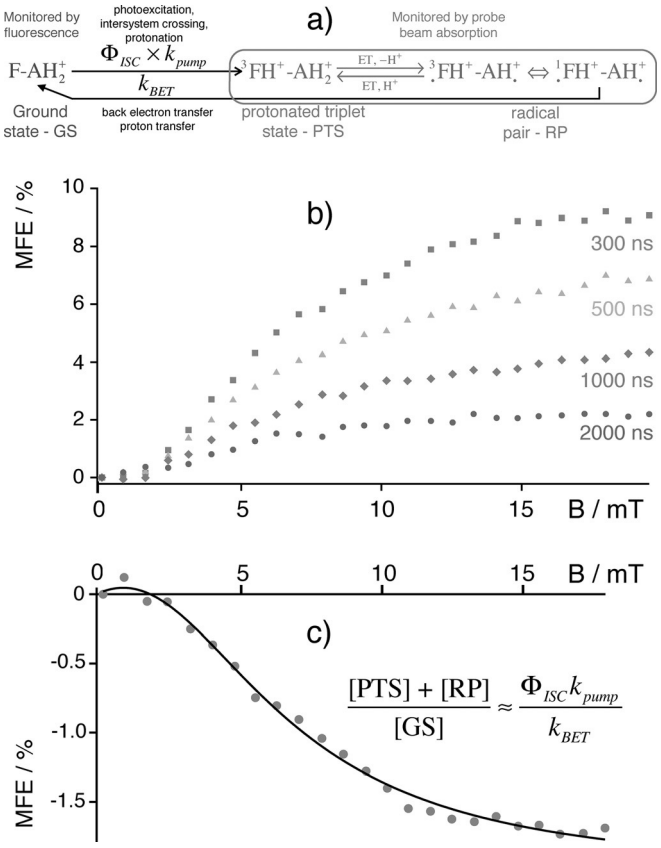

Figure 4. a) Simplified reaction scheme for FAD photoexcitation at pH 2.3. b) Reduction of the MFE on RP/PTS concentration with increasing pump light pulse length. c) Singlet excited state FAD fluorescence detected MARY curve under high power CW pump light modulation, revealing an inverse MFE on the FAD GS concentration.

a positive or negative MFE depending on which state is observed and the intensity of the irradiation light.

We have demonstrated for the first time the techniques of TOAD microscopy, which allows direct imaging of photochemically generated radicals, and MIM microscopy, which can selectively image regions containing magnetically sensitive RPs. The techniques have both submicrometer spatial resolution and high sensitivity, as demonstrated by the ability to rapidly record images and MARY curves by irradiating a 200 μM FAD sample of less than 4 fL. This means that even when spatial resolution is unnecessary, the instrument can be employed as a high sensitivity spectroscope that can operate on (for example precious biological) samples of less than 1 μL, and by scanning the total sample area allow progressive photoexcitation of unirradiated sample, analogous to sample flow in a conventional cuvette. In addition, a LFE on FAD photochemistry was resolved for the first time, and the shift of MFE from RP to FAD GS under cycling conditions was also clearly observed. These features are both important for the understanding of magnetoreception in cryptochromes. TOAD and MIM measurements on both plant and animal cells and tissues, and MFE measurements on pure cryptochrome protein in solution are currently underway.

Experimental Section

FAD was purchased from Wako and used as received. pH 2.3 buffer solution was made by combining citric acid and disodium hydrogen phosphate solutions (Wako) in distilled water (Wako).[13] Thin samples were produced by adding polymer microbeads (diameter 2.5–2.9 μm, Spherotech Inc.) to the sample solution and sandwiching 1 μL of this solution between glass cover slips (0.13–0.16 mm, Marienfeld). For thicker samples, the polymer beads were replaced with 100 μm glass beads (Toshin Riko) and the volume of solution increased to 5 μL.

Keywords: absorption · laser spectroscopy · photochemistry · radicals · reactive intermediates

How to cite: *Angew. Chem. Int. Ed.* **2015**, *54*, 8494–8497
Angew. Chem. **2015**, *127*, 8614–8617

[1] U. E. Steiner, T. Ulrich, *Chem. Rev.* **1989**, *89*, 51–147.
[2] J. R. Woodward, *Prog. React. Kinet. Mech.* **2002**, *27*, 165–207.
[3] C. T. Rodgers, *Pure Appl. Chem.* **2009**, *81*, 19–43.
[4] H. Mouritsen, P. J. Hore, *Curr. Opin. Neurobiol.* **2012**, *22*, 343–352.
[5] E. Ehrenfreund, Z. V. Vardeny, *Organic Spintronics*, CRC, Boca Raton, **2010**, pp. 217–255.
[6] H. Lee, N. Yang, A. E. Cohen, *Nano Lett.* **2011**, *11*, 5367–5372.
[7] C. A. Combs, *Curr. Protoc. Neurosci.* **2001**, *2*.1.1–2.1.14.
[8] P. Kukura, M. Celebrano, A. Renn, V. Sandoghdar, *J. Phys. Chem. Lett.* **2010**, *1*, 3323–3327.
[9] M. Celebrano, P. Kukura, A. Renn, V. Sandoghdar, *Nat. Photonics* **2011**, *5*, 95–98.
[10] M. Murakami, K. Maeda, T. Arai, *Chem. Phys. Lett.* **2002**, *362*, 123–129.
[11] M. Murakami, K. Maeda, T. Arai, *J. Phys. Chem. A* **2005**, *109*, 5793–5800.
[12] S. R. T. Neil, J. Li, D. M. W. Sheppard, J. Storey, K. Maeda, K. B. Henbest, P. J. Hore, C. R. Timmel, S. R. Mackenzie, *J. Phys. Chem. B* **2014**, *118*, 4177–4184.
[13] T. C. McIlvaine, *J. Biol. Chem.* **1921**, *49*, 183–186.

Received: March 20, 2015
Published online: June 3, 2015

